DOSIMETRY OF SMALL PERIPHERAL LUNG CANCER WITH GROUND-GLASS OPACITY IN RADIOTHERAPY USING A PHANTOM MODEL AND RADIOCHROMIC FILM

Ujifuku. A*, Katsuda. T**, Gotanda. R* Inamura. K***, Kawabe. A*, Nakagiri. Y**

*Graduate School of Health Science, Okayama University, Okayama, Japan
**Faculty of Health Sciences, Okayama University Medical School, Okayama, Japan
*** Okayama University Hospital, Okayama, Japan

angie150703@yahoo.co.jp

Abstract: Many small peripheral lung cancer lesions with ground- glass opacity (GGO) are detected by computed tomographic (CT) scanning of the chest. In radiotherapy for GGO tumors, a lack of build-up in the tumor occurs due to its low-density and the tumor dose may not be delivered sufficiently to accomplish treatment. To accurately measure the tumor dose delivery, radiochromic films, a thoracic model and tumor phantoms were used. Normally, the tumor dose is increased by build-up in the tumor and this increase is caused by the tumor size and density. Therefore, in radiotherapy for the lung with GGO tumor, sufficient build up in the tumor may not occur. Furthermore, the build-down as the beam exits the surface of the GGO phantom was less than that of the Nodule phantom. When an ideal dose was delivered to the GGO phantom, the lung might have been overexposed. Careful planning is required for the precise management of the absorbed dose of GGO tumors during radiotherapy.

Introduction

In radiotherapy of lung cancer, it is difficult to determine the absorbed dose of small lung tumor because of the low density of the lung. The lung density is about 0.3 g/cm^3, which is different from the human soft-tissue density [1]. Therefore, the number of recoil electrons per unit volume in the lung is smaller than that of the soft-tissue. Thus, secondary scattered radiation doses are also lesser. Furthermore, if the tumor is of a certain size, the build-up is sufficient for radiotherapy. For GGO tumor, the lack of build-up in the tumor occurs due to its low-density and the tumor dose may not be delivered sufficiently to accomplish radiotherapy. In this study, the accuracy of tumor dose delivery is evaluated. To measure the absorbed dose distribution in the lung and the tumor using radiochromic film, thoracic and tumor model phantoms were constructed.

Materials and Methods

The calibration curve of GAFCHROMIC HS film (HS-film)

Recently, many kinds of radiochromic film (RCF), named GAFCHROMIC film, have become available. The RCF is self-developing radiation sensitive [2]. Thus, it does not need any post exposure processing. When it is exposed to radiation, it reacts to form a blue color. The absorbed dose can be obtained from its density growth. To measure the absorbed dose, tissue-equivalent HS-film was applied. This was suitable for the measurement of high energy radiation.

A calibration curve to convert the density to the absorbed dose is necessary with HS-film dosimetry. For this experiment, 1.5 cm x 1.5 cm size film pieces were cut from a 5 inch x 5 inch sheet. These films were embedded between 5 cm thickness water equivalent phantoms. Exposure parameters were 10 MV X-ray, Monitor Units corresponded to 1-15 Gy on the films, calculated by 3D-RTPS, FOCUS Release 2.5.0 (Computerized Medical System, Inc. MO), 300 cGy/min, 10 cm x 10 cm field size and source – the film distance was 100 cm. The linear accelerator (MEVATRON 77 DX67, Siemens, Munich) was used. A schematic diagram of the exposure arrangement is shown in figure 1.

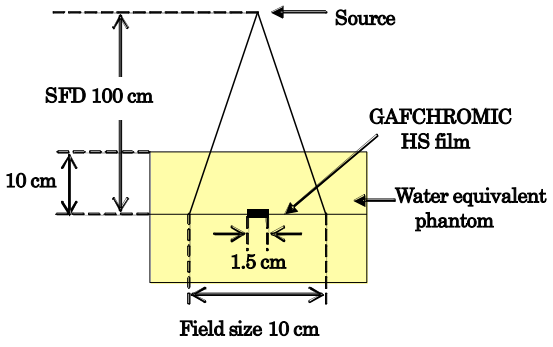

Figure 1: Exposure arrangement to generate the calibration curve.

The thoracic model and tumor phantoms

The thoracic model phantom was consisted of three layers. A 15 cm cork layer (lung) was placed between 3 cm (front chest wall) and 5 cm (back chest wall) water equivalent phantom layers. The density of the cork was 0.25 g/cm^3 and the water equivalent phantom was 1.04 g/cm^3. The thoracic model phantom was exposed to the

ISSN: 1727-1983

10 MV photon beam to generate the absorbed dose curve along the beam axis.

Two density types of tumor phantoms, GGO phantom and Nodule phantom, were constructed. In each type, two lesion sizes 1 x 1 x 1 cm^3 and 2 x 2 x 2 cm^3 were constructed (figure 2). The Nodule phantoms were made of Mix-DP. The GGO phantoms were made of mixed Mix-DP and cork. Densities were deduced from the CT numbers of the Nodule phantoms 1.04 g/cm^3 and the GGO phantoms 0.74 g/cm^3 (figure 3). These phantoms could be embedded in the thoracic model phantom (figure 4).

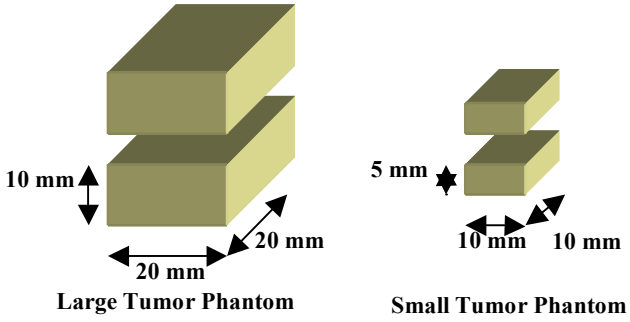

Figure 2: Schematic diagrams of tumor phantoms.

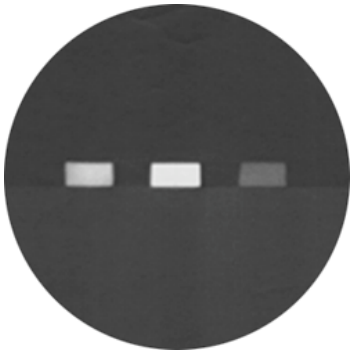

Figure 3: CT image of phantoms.
Left: GGO phantom
Center: Nodule phantom
Right: cork

Exposure parameters for the thoracic model phantom

The HS-films (1.5 cm x 1.5 cm) were embedded along with the beam axial direction in the thoracic model phantom. The X-ray entrance face of the thoracic model phantom was set to a depth of 0 cm. These films were embedded from 0 cm to 23 cm depths, with distances of 1 cm between each. An additional film was set at a depth of 3.5 cm for an anticipated dose increment due to the build-up effect. A total of 25 HS-film pieces were used. For the exposure, the linear accelerator (MEVATRON 77 DX67, Siemens, Munich) was used. The exposure parameters were 10 MV X-ray, the Monitor Units corresponded to 5 Gy to the center of the 23 cm water equivalent phantom thickness, calculated with 3D-RTPS, FOCUS Release 2.5.0 (Computerized Medical System, Inc. MO), 300 cGy/min, 5 cm x 5 cm field size, the isocenter was 11.5 cm in depth for the thoracic model phantom and the source - isocenter distance was 100 cm.

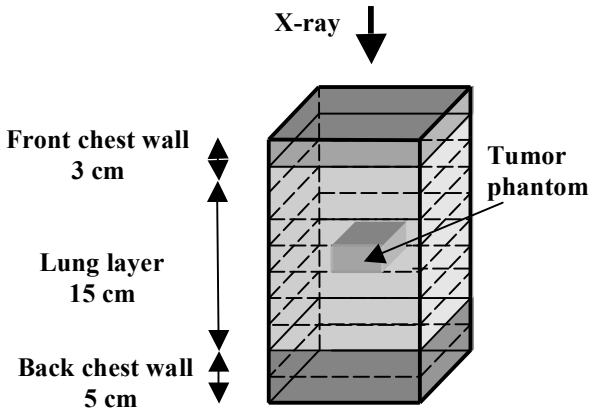

Figure 4: Thoracic model phantom for dosimetry.

Exposure parameters for the tumor phantoms

Tumor phantoms were embedded in the thoracic model at a depth of 11.5 cm, and exposure parameters were as same as for the thoracic model phantom. With the small tumor phantoms, the films were set of depths of 0 cm to 23 cm with distances of 1 cm between each. There was an additional film in the tumor phantom placed at a depth of 11.5 cm. Positions at depths of 11 cm, 11.5 cm and 12 cm were placed on both sides of the small tumor phantoms and at the center of them. With the large tumor phantoms, the films were set from depths of 0 cm to 10 cm and from 13 cm to 23 cm with distances of 1 cm between each. Film positions at 10.5 cm, 11.5 cm and 12.5 cm depth were placed on both sides and at the center of the large tumor phantoms.

HS-film dosimetry

Films were scanned prior to exposure and 48 hours after exposure with a flat-bed color scanner (EPSON ES-2200, Seiko Epson Co. Nagano). For analysis, the pixel values of the red mode image were selected from the RGB image to maximize the density response. The response of the HS-film density is maximized to use red pixel values [3]. There were many artifacts caused by scratches, dust and cutting of the surface. It was therefore necessary before and after exposure to process the images for artifact removal with image analysis software, Adobe Photoshop 6.0 (Adobe, CA) and National Institutes of Health (NIH) Image 1.62b (NIH, Maryland). Advantage pixel values of each film were calculated. After that, the mean pixel value of the images before exposure was subtracted from that of the images after exposure. The pixel value after subtraction processing is called the net pixel value (NPV). The NPV of each film was measured. Then, the original film response was obtained.

ISSN: 1727-1983

Results

Figure 5 shows the calibration curve of the NPV and absorbed dose. This calibration curve was used for all data analysis of the following results.

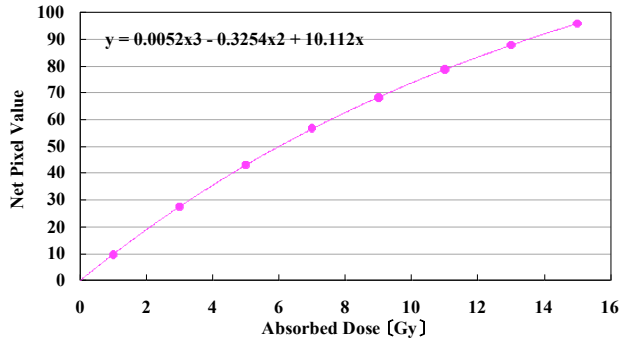

Figure 5: The calibration curve of HS-film.

Figure 6 shows the absorbed dose curves in the thoracic model phantom with or without small tumor phantoms. Absorbed doses at depths of 11 cm, 11.5 cm and 12 cm are shown in table 1. These doses were at the front face, the center and the back face of the small tumor phantoms. With the GGO phantom, the absorbed doses were 5.32 Gy at 11 cm depth, 5.30 Gy at 11.5 cm depth and 5.32 Gy at 12 cm depth. These doses were increased -0.2 %, 0.2 % and 1.5 % compared to those doses without tumor phantoms. With the Nodule phantom, the absorbed doses were 5.25 Gy at 11 cm depth, 5.25 Gy at 11.5 cm depth and 5.35 Gy at 12 cm depth. These doses were increased -1.5 %, -0.9 % and 2.1 %, respectively, compared to those doses without tumor phantoms.

A build-up in the front chest wall occurred and a build-down in the lung was observed in all curves. In the pre-tumor area, the three curves almost overlapped. Without tumor phantoms, the absorbed dose only decreased in the lung area. Using tumor phantoms, a rebuild-up was observed in the tumor. The dose in the GGO phantom was showed a lower increase than that in the Nodule phantom. Thereafter, the rebuild-down was observed at the posterior portion of both the tumor phantoms. Therefore, the two absorbed dose curves intersected with or without tumor phantoms at a depth of about 13 cm. At the back chest wall, the absorbed dose increments caused by rebuild-up were observed for all curves.

Figure 7 showed absorbed dose curves with or without large tumor phantoms. Absorbed doses at depths of 10.5 cm, 11.5 cm and 12.5 cm were shown in table 2. These doses were at the front face, the center and the back face of the large tumor phantoms. With the GGO phantom, the absorbed doses were 5.37 Gy at 10.5 cm depth, 5.52 Gy at 11.5 cm depth and 5.37 Gy at 12.5 cm depth. These doses were increased -0.7 %, 4.3 % and 3.5 %, respectively, compared to those without tumor phantoms. With the Nodule phantom, the absorbed doses were 5.50 Gy at 10.5 cm depth, 5.71 Gy at 11.5 cm depth and 5.31 Gy at 12.5 cm depth. These doses were increased 1.7 %, 7.9 % and 2.3 % compared to those without tumor phantoms.

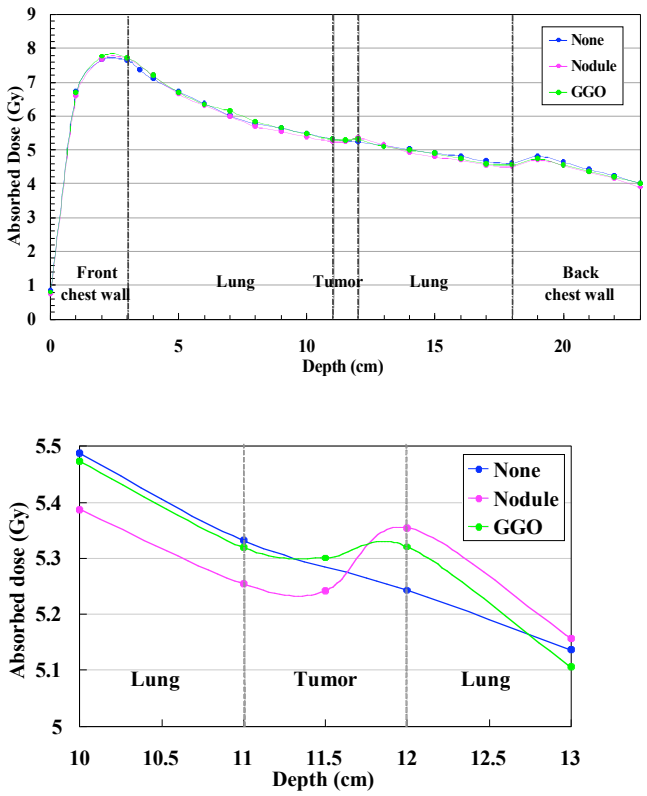

Figure 6: Absorbed dose curves with or without small tumor phantoms in thoracic model phantom (upper). Absorbed dose curves enlarged around the tumor phantoms (lower).

Table 1: Absorbed dose

Depth (cm)	None (Gy)	GGO (Gy)	Nodule (Gy)
11	5.33	5.32 (-0.2 %)	5.25 (-1.5%)
11.5	5.29	5.30 (0.2 %)	5.25 (-0.9%)
12	5.24	5.32 (1.5 %)	5.35 (2.1%)

GGO: ground-glass opacity

Behaviors of the absorbed curves were similar to those for small tumor phantoms, but they have greater dose variation. A build up in the front chest wall and build-down in the lung was observed in all curves. In the pre-tumor area, the three curves almost overlapped. With the large tumor phantoms, rebuild-up was observed in the tumor phantoms. The dose in the GGO phantom showed a lower increase than that in the Nodule phantom. Thereafter, a rebuild-down was observed at the posterior portion of the tumor. A dose decrement occurred notably in the Nodule phantom. In the back chest wall, the absorbed dose increments, caused by rebuild-up, were observed for all curves.

ISSN: 1727-1983

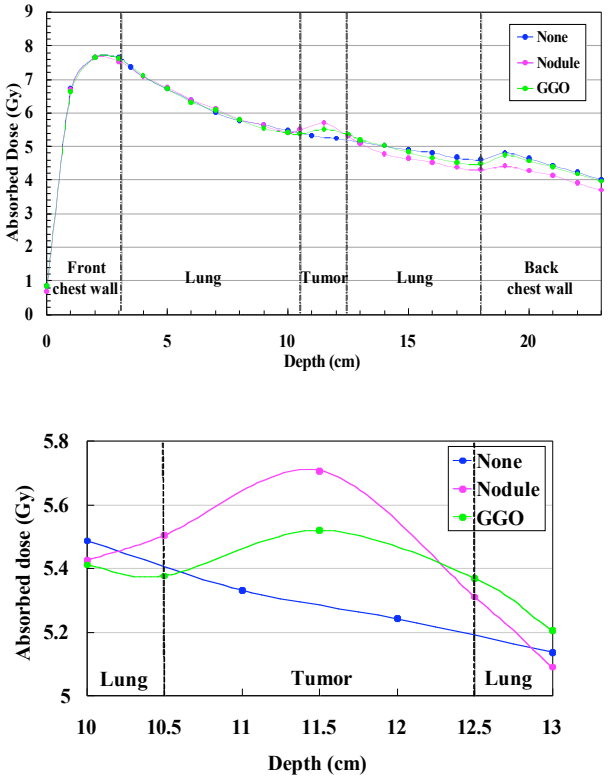

Figure 7: Absorbed dose curves with or without large tumor phantoms in thoracic model phantom (upper). Absorbed dose curves enlarged around the tumor phantoms (lower).

Table 2: Absorbed dose.

Depth (cm)	None (Gy)	GGO (Gy)	Nodule (Gy)
10.5	5.41	5.37 (-0.7 %)	5.50 (1.7%)
11.5	5.29	5.52 (4.3 %)	5.71 (7.9%)
12.5	5.19	5.37 (3.5 %)	5.31 (2.3%)

GGO: ground-glass opacity

Discussion

Build-up occurs when high energy X-rays are incident from low density materials to high density materials. The dose increment occurs at the interface between them by secondary scattering. Build-down means a decreasing dose, the opposite phenomenon of build-up.

The three absorbed dose curves almost overlapped in the front chest wall and the front lung area until reaching the small tumor phantoms. In the tumor area, the absorbed dose curve without tumor phantoms only showed a decline. When using tumor phantoms; however, an increasing dose was observed in this area. The dose increasing rate in the Nodule phantom is larger than that of the GGO phantom. With the Nodule phantom, this increase due to build-up reached a peak at the depth of the tumor back face. With the GGO phantom, the absorbed dose decreased a little at the center of tumor, but the dose increase due to build-up occurred at the depth of the tumor back face. Ultimately, the absorbed dose in the GGO tumor phantom remined almost flat. When using tumor phantoms, dose decrease due to build-down occurred in the back lung area. Therefore, two curves with small tumor phantoms intersected with those with no tumor phantoms. At the entrance face to the back chest wall, the build-up phenomenon was observed in all curves. At a depth of about 12 cm, was considered to be a build-up peak in the small tumor phantoms. When those without tumor phantoms were standardized, the dose increase rate in the GGO and the Nodule phantoms at a depth of 12 cm as the build-up peak in the small tumor phantoms were 1.5% and 2.1%, respectively. It was found that the rate of increase in the GGO phantom was smaller than that of the Nodule phantom.

When using large tumor phantoms, the absorbed dose curves were similar to those of the small tumor phantoms. The three curves almost overlapped in the front chest wall and the front lung area. In the tumor area, the dose increase due to build-up was observed when using both tumor phantoms. This rate of increase in the Nodule phantom was higher than that of the GGO phantom. Both build-up peaks in the GGO and the Nodule tumor phantoms were observed at a depth of 11.5 cm (i.e. the center of tumor phantoms). In the back lung area, the dose decrease due to build-down occurred when tumor phantoms were used. The dose decrease occurred on a larger scale in the Nodule phantom. At the back face of the tumor phantom, the absorbed dose of the GGO phantom was higher than that of the Nodule phantom. At the entrance surface of the back chest wall, the build-up phenomenon was observed in all curves. The dose increase rate in the GGO and the Nodule phantoms at a depth of 11.5 cm (i.e. the build-up peak in the large tumor phantoms) were 4.3% and 7.9%, respectively. It was found that the rate of increase in the GGO phantom was clearly lower than that of the Nodule phantom. It is predictable that the dose increase due to build-up occurred in the tumor. In the GGO phantom, its low-density gave a lower dose growth.

The absorbed dose increase due to the build-up in the large tumor phantom was higher than that in small tumor phantom. Additionally, the dose increase in the Nodule phantom was higher than that in the GGO phantom. It was found that the increase of tumor size and density was related to the increase in the scale of the build-up in the tumor. Thus, in the case of radiotherapy, the lack of build-up in a GGO tumor may occur. A sufficient dose to the tumor dose to accomplish radiotherapy may therefore not be delivered.

As with the absorbed dose curves with the large tumor phantom, the absorbed dose with the GGO phantom was higher than that of the Nodule phantom in the back lung area. In radiotherapy of the lung, the bilateral irradiation method is used. However, the single field irradiation method was used this experiment. If the bilateral irradiation method was used, the same phenomenon of the build-up and the build-down will

ISSN: 1727-1983

also occur in the reverse direction. It is considered that the difference of tumor dose between the GGO phantom and the Nodule phantom will be wider. Additionally, the build-down from the tumor to the lung will occur at the front and back surface of the tumor, depending on the beam directions. The build-down with the Nodule phantom is bigger than that of the GGO phantom. Thus, in case of the radiotherapy for the GGO tumor, the exposure dose of the lung will be higher than that with the nodule tumor. For the radiotherapy of the GGO tumor, there is a concern that there may be a lack of the dose to the tumor or an overdose to the lung.

Conclusions

When the absorbed dose curve without tumor phantoms is standardized, the rate of increase of the peak absorbed dose in the four tumor phantoms, small GGO, small Nodule, large GGO and large Nodule were 1.5%, 2.1%, 4.3% and 7.9%, respectively.

Normally, the tumor dose is increased by build-up in the tumor and this increase is caused by the tumor size and density. Therefore, in radiotherapy for the lung with the GGO tumor, a sufficient build-up in the tumor may not occur. Furthermore, the build-down as the beam exits the surface of the GGO phantom was smaller than that of the Nodule phantom. When an ideal dose was delivered to the GGO phantom, the lung may be overexposed. Careful planning is required for the precise management of the absorbed dose of GGO tumors during radiotherapy.

References

[1] DYK J, BATTISTA JJ, RIDER WD. (1980): Half body radiotherapy: the use of computed tomography to determine the dose to lung', Int. J. Radiat. Oncol. Biol. Phys., 6, pp. 463-470

[2] NIROOMAN-RAD A, BLACKWELL C. R, COURSEY B. M. (1998): 'Radiochromic film dosimetry. Recommendations of AAPM Radiation Therapy Committee Task Group 55', Med. Phys., 25, pp. 2093-2115

[3] ISP, Internet site address: http://www.ispcorp.com/products/dosimetry/index.html

ISSN: 1727-1983